mononegative X^{n-} but now suggesting the presence of some ion-pair character in the transition state when $X^{n-} = SO_4^{2-}$, as noted above. This latter effect is less marked at the higher ionic strength, as expected for ion association.[8]

The Volume Profile Concept. The final column of Table III lists values of a parameter V_c^R which is analogous to Palmer and Kelm's V_R except that it is conventional rather than an absolute molal volume.

$$V_c^R = V_c(Co(NH_3)_5X^{(3-n)+}) + \Delta V^*_0 - V_c(X^{n-}) \quad (12)$$

This would equal the partial molal volume of an intermediate $\{Co(NH_3)_5^{3+}\}^*$ if an extreme dissociative (D) mechanism were operating, i.e., if X^{n-} were lost completely in the transition state and consequently had its normal bulk-solution molal volume. If, however, the mechanism of reaction 1 is dissociative interchange (I_d), as seems likely,[15] X^{n-} will be present in the outer sphere of $Co(NH_3)_5^{3+}$ with a molal volume appropriate to such an environment; thus, for $X^{n-} = H_2O$, $V_c(X^{n-})$ should be about 15 rather than 18 cm^3 mol^{-1}.[1,4,18] The modest spread in V_c^R values in Table III is therefore quite consistent with an I_d process, especially since the more deviant sulfato case can be understood as explained above. In particular, it is now clear that the case of aqua exchange in reaction 1 ($X^{n-} = H_2O$) is entirely compatible with the others, whether one chooses $V_c(H_2O)$ to be 15 or 18 cm^3 mol^{-1}; the zero value adopted in ref 5 is quite inappropriate. The use of the volume-profile approach, as advocated by Palmer and Kelm,[5] is vindicated by the present study, but is now seen to be less clear-cut than one would like, especially in view of the potential for error in V_c values for the complex ions.

If we take the aqua exchange case as being most likely to give a realistic value of $V_c(Co(NH_3)_5^{3+})$, this can be set at 53–56 cm^3 mol^{-1} on the *conventional* scale; this is 17–20 cm^3 mol^{-1} smaller than V_c for $Co(NH_3)_6^{3+}$ (Table II). We conclude that *Stranks' postulate*,[4] that these two quantities can be taken as equal, *is in error by an amount that exceeds most of the values of* $|\Delta V|$ *and* $|\Delta V^*_0|$ *so far recorded for reaction 1 and related series and must never be used in attempting to rationalize such values.*

We can infer from this that the effective molar volume of an ammine ligand coordinated to cobalt(III) is 17–20 cm^3 mol^{-1}, whereas ϕ_v for NH_3 may be calculated from density data[31] for aqueous ammonia to be 24.5 cm^3 mol^{-1}. Thus, the upper limit of ΔV^* for the $Co(NH_3)_6^{3+}$–NH_3 exchange reaction may be set at +7.5 cm^3 mol^{-1} for a D mechanism. Interestingly, in 1924, Birk and Biltz[32] used the densities of solid halides to estimate that the average molal volume of a coordinated ammonia in $M(NH_3)_6^{3+}$ (M = Co, Cr) is 20 cm^3 mol^{-1}. Molar volumes of neutral ligands calculated from the densities of solids should be regarded only as upper limits for the solution values because of the effect of empty space in the lattice in some cases on the measured density; for example, the molar volume of ice-I_h is 19.6 cm^3 mol^{-1}, as against 9.0 for the hypothetical closest packed structure,[33] while Birk and Biltz's "gleichräumiger Verbindungen" $[M(NH_3)_6]X_2$ and $[M(NH_3)_6]X_3$, in which interstices in the quasi-antifluorite lattice of the former are filled with additional anions X^- in the latter[34] to give equal apparent molar volumes,[32] provide fair warning. Nevertheless, the agreement between the present approach and that of Birk and Biltz is encouraging.

Acknowledgment. We thank the Natural Sciences and Engineering Research Council of Canada for financial assistance, the Province of Alberta for a Graduate Fellowship (to M.J.S.), and Professor H. Kelm for discussions.

Registry No. $[Co(NH_3)_6](ClO_4)_3$, 13820-83-2; $[Co(NH_3)_5OH_2](ClO_4)_3$, 13820-81-0; $[Co(NH_3)_5Cl](ClO_4)_2$, 15156-18-0; $[Co(NH_3)_5Br](ClO_4)_2$, 14591-65-2; $[Co(NH_3)_5SO_4]ClO_4$, 15156-23-7; $[Co(NH_3)_5NCS](ClO_4)_2$, 15663-42-0; $[Co(NH_3)_5N_3](ClO_4)_2$, 14283-04-6; $[Cr(NH_3)_5OH_2](ClO_4)_3$, 32700-25-7; $[Cr(NH_3)_5OH_2](NO_3)_3$, 19683-62-6; $[Cr(NH_3)_5Cl](ClO_4)_2$, 22478-30-4; $Co(NH_3)_5HSO_4^{2+}$, 15156-26-0; HCl, 7647-01-0; $HClO_4$, 7601-90-3.

Supplementary Material Available: A table showing the dependence of pseudo-first-order rate coefficients k_{obsd} for the aquation of $Co(NH_3)_5SO_4^+$ on temperature, pressure, and acidity (2 pages). Ordering information is given on any current masthead page.

(31) Weast, R. C., Ed. "Handbook of Chemistry and Physics", 56th ed.; Chemical Rubber Publishing Co.: Cleveland, OH, 1975; p D221.
(32) Birk, E.; Biltz, W. *Z. Anorg. Allg. Chem.* **1924**, *134*, 125.
(33) Swaddle, T. W. *Inorg. Chem.* **1980**, *19*, 3203; *Rev. Phys. Chem. Jpn.* **1980**, *50*, 230.
(34) Wells, A. F. "Structural Inorganic Chemistry", 4th ed.; Oxford University Press: London, 1975.

Contribution from the Laboratoire de Chimie Quantique, ER No. 139 du CNRS, Institut Le Bel, Université Louis Pasteur, 67000 Strasbourg, France

Theoretical Study of the Olefin Insertion Step in the Chlorotris(triphenylphosphine)rhodium(I)-Catalyzed Hydrogenation of Olefins

A. DEDIEU

Received January 15, 1981

Ab initio LCAO–MO–SCF calculations have been performed for the reaction $H_2RhCl(PH_3)_2(C_2H_4) \rightarrow HRhCl(PH_3)_2(C_2H_5)$. This reaction stands as a model for the first hydrogen transfer in the dihydrido olefinic intermediate involved in the $RhCl(PPh_3)_3$-catalyzed hydrogenation of olefins. It is found that the early stages of the process, up to the transition state, are best described as an ethylene insertion into the Rh–H bond. The calculations indicate that some polytopal rearrangements occur simultaneously with relaxation from the transition state. The whole insertion process is computed to be exothermic with a rather moderate energy barrier. In connection with the origin of this barrier the metal substitution pattern is discussed. The presence of a good π-donor ligand in the coordination sphere promotes the olefin insertion, as opposed to the hydrogen migration, and lowers the energy barrier. Finally, the directionality of the insertion for some substituted olefins is analyzed on the basis of the composition of the perturbed molecular orbitals.

Introduction

We recently undertook[1,2] a theoretical study of the hydrogenation of olefins catalyzed by the chlorotris(triphenylphosphine)rhodium(I) complex (the so-called Wilkinson complex $RhCl(PPh_3)_3$).[3] The key intermediate of the corresponding catalytic cycle is an octahedral dihydrido olefinic

(1) Dedieu, A. *Inorg. Chem.* **1980**, *19*, 375.
(2) Dedieu, A.; Strich, A. *Inorg. Chem.* **1979**, *18*, 2940.
(3) (a) Jardine, F. H.; Osborn, J. A.; Wilkinson, G.; Young, J. F. *Chem. Ind. (London)* **1965**, 560. (b) Bennett, M. A.; Longstaff, P. A.; *Ibid.* **1965**, 846. (c) Osborn, J. A.; Jardine, F. H.; Young, J. F.; Wilkinson, G. *J. Chem. Soc. A* **1966**, 1711.

0020-1669/81/1320-2803$01.25/0

complex H_2RhClL_2(olefin) (L = PPh_3) in which the two hydrogen atoms are transferred stepwise.[4,5] The first transfer, giving rise to the hydridoalkyl intermediate $HRhClL_2$(alkyl) is generally believed to be the rate-determining step of the whole process.[6-9] This hydrogen 1,2 shift (eq 1) between the

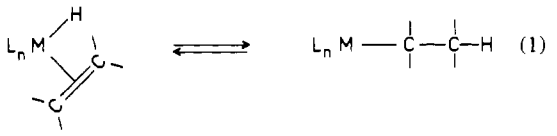

(1)

metal and a coordinated olefin is a well-established reaction of the organometallic area.[11] It has also been postulated in several other homogeneous catalytic processes.[12] The precise mechanism of this step is unknown however, since the H_2RhClL_2(olefin) and the $HRhClL_2$(alkyl) intermediates have not been observed directly by spectroscopic techniques. Recently some dihydrido(olefin)iridium complexes related to the H_2RhClL_2(olefin) system have been isolated and their structure deduced from NMR and IR spectra.[13-15] A hydrido(alkyl)rhodium intermediate in a homogeneous catalytic hydrogenation reaction has been intercepted and characterized through NMR.[16,17] Only a few equilibria between an hydrido(alkene)metal complex and an alkylmetal complex have been observed through NMR spectra.[18-21]

Theoretical analyses have now increased our understanding of the olefin insertion reaction into a d^8 metal–hydrogen bond[22-25] or of the Ziegler–Natta-type process,[26-31] most of them using semiempirical techniques.[22,23,25-29,31] But no investigation of this type has been devoted to reaction 1 in a d^6 metal complex. We present here a theoretical study of the hydrogen-transfer step in the d^6 dihydrido olefinic intermediate H_2RhClL_2(olefin) using LCAO–MO–SCF calculations. Our first goal was to determine the stereochemistry of the transfer, whether it is a hydride migration or an olefin insertion, to characterize the transition state (if any), and hence to single out the factors governing the ease of the reaction. We then extend our study to a molecular orbital analysis of some substitution effects.

Calculations

LCAO–MO–SCF ab initio calculations have been carried out on reaction 2, where L = PH_3, C_2H_4, and C_2H_5 stand as models for the

$$H_2RhClL_2(C_2H_4) \rightarrow HRhClL_2(C_2H_5) \quad (2)$$

triphenylphosphine, the olefin, and the alkyl ligands, respectively. The Rh–Cl, Rh–P, and Rh–H distances were set to 2.40, 2.37, and 1.65 Å, respectively.[32] The geometries of the coordinated C_2H_4 (**1**) and

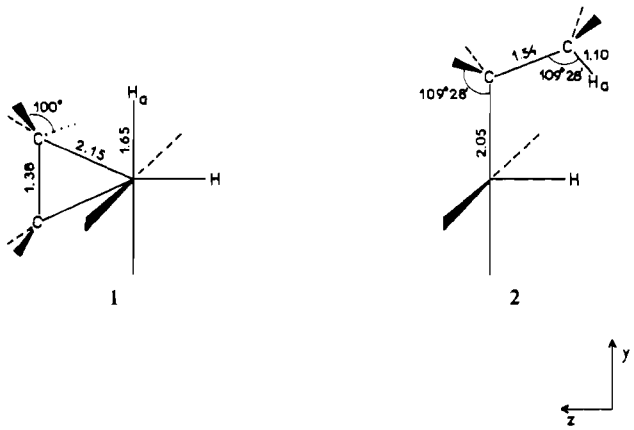

1 2

C_2H_5 (**2**) ligands are shown.[32,33] For the PH_3 ligand the experimental geometry was chosen.[34] Bond distances, other than the Rh–H_a, Rh–C, and C–C bond distances, were kept set to their original values throughout the transfer process. Also the C_s symmetry of the system was maintained.

Calculations were carried out with the system of programs ASTERIX[35] with use of the following Gaussian basis sets: (13,9,7) contracted to [5,4,3] for Rh;[36] (10,6) contracted to [4,3] for phosphorus and chlorine,[37] (8,4) contracted to [3,2] for the first-row atoms;[38] (4) contracted to [2] for hydrogen[39] (the contracted basis set is a minimal set for the inner shells, the 5s and 5p shells of rhodium, and a double-ζ set for the valence shells).

Results

We first need to review breifly our previous conclusions.[1] Two stereoisomers (**3a** and **3b**) of the dihydrido olefinic in-

(4) Bond, G. C.; Hillyard, R. A. *Discuss. Faraday Soc.* **1968**, *46*, 20.
(5) (a) Hussey, A. S.; Takeuchi, Y. *J. Am. Chem. Soc.* **1969**, *91*, 672. (b) Hussey, A. S.; Takeuchi, Y. *J. Org. Chem.* **1970**, *35*, 643.
(6) Siegel, S.; Ohrt, D. *Inorg. Nucl. Chem. Lett.* **1972**, *8*, 15.
(7) Halpern, J.; Okamoto, T.; Zakhariev, A. *J. Mol. Catal.* **1976**, *2*, 65.
(8) Ohtani, Y.; Fujimoto, M.; Yamagishi, A. *Bull. Chem. Soc. Jpn.* **1977**, *50*, 1453; **1979**, *52*, 69.
(9) It has been claimed however that the formation of the dihydrido olefinic intermediate is the rate-determining step.[10]
(10) De Croon, M. H. J. M.; van Nisselrooij, P. F. M. T.; Kuipers, H. J. A. M.; Coenen, J. W. E. *J. Mol. Catal.* **1978**, *4*, 325.
(11) (a) Cramer, R. *J. Am. Chem. Soc.* **1966**, *88*, 2272. (b) Cramer, R.; Lindsey, R. V. *Ibid.* **1966**, *88*, 3534.
(12) See, for instance: Henrici-Olivé, G.; Olivé, S. *Top. Curr. Chem.* **1976**, *67*, 107.
(13) Crabtree, R. H.; Felkin, H.; Morris, G. E. *J. Chem. Soc., Chem. Commun.* **1976**, 716.
(14) Crabtree, R. H.; Felkin, H.; Fillebeen-Khan, T.; Morris, G. E. *J. Organomet. Chem.* **1979**, *168*, 183.
(15) Hietkamp, S.; Stufkens, D. J.; Vrieze, K. *J. Organomet. Chem.* **1978**, *152*, 347.
(16) Chan, A. S. C.; Halpern, J. *J. Am. Chem. Soc.* **1980**, *102*, 838.
(17) This hydrogenation reaction involves the cationic rhodium catalyst Rh(diphos)$^+$ (diphos = 1,2-bis(diphenylphosphino)ethane).
(18) Byrne, J. W.; Blaser, H. V.; Osborn, J. A. *J. Am. Chem. Soc.* **1975**, *97*, 3871.
(19) Seiwell, L. P. *Inorg. Chem.* **1976**, *15*, 2560.
(20) Chaudret, B. N.; Cole-Hamilton, D. J.; Wilkinson, G. *Acta Chem. Scand., Ser. A* **1978**, *A32*, 763.
(21) Werner, H.; Feser, R. *Angew, Chem., Int. Ed. Engl.* **1979**, *18*, 157.
(22) Wheelock, K. S.; Nelson, J. H.; Kelly, J. D.; Jonassen, H. B.; Cusachs, L. C. *J. Chem. Soc., Dalton Trans.* **1973**, 1457.
(23) Sakaki, S.; Kato, H.; Hanai, H.; Tamara, K. *Bull. Chem. Soc. Jpn.* **1975**, *48*, 813.
(24) Grima, J. Ph.; Choplin, F.; Kaufmann, G. *J. Organomet. Chem.* **1977**, *129*, 221.
(25) Thorn, D. L.; Hoffmann, R. *J. Am. Chem. Soc.* **1978**, *100*, 2079.
(26) (a) Amstrong, D. R.; Perkins, P. G.; Stewart, J. P. *J. Chem. Soc., Dalton Trans.* **1972**, 1972. (b) Amstrong, D. R.; Fortune, R.; Perkins, P. G. *J. Catal.* **1976**, *42*, 435.
(27) Novaro, O.; Chow, S.; Magnonat, P. *J. Catal.* **1976**, *41*, 91.
(28) Lauher, J. W.; Hoffmann, R. *J. Am. Chem. Soc.* **1976**, *98*, 1729.
(29) (a) Giunchi, G.; Clementi, E.; Ruiz-Vizcaya, M. E.; Novaro, O. *Chem. Phys. Lett.* **1977**, *49*, 8. (b) Novaro, O; Blaisten-Barojas, E.; Clementi, E.; Giunchi, S.; Ruiz-Vizcaya, M. E. *J. Chem. Phys.* **1978**, *68*, 2337.
(30) Cassoux, P.; Crasnier, F.; Labarre, J. F. *J. Organomet. Chem.* **1979**, *165*, 303.
(31) McKinney, R. J. *J. Chem. Soc., Chem. Commun.* **1980**, 490.
(32) (a) See ref 1 for references of related structures. (b) An X-ray crystal structure of an IrH_2ClL_2(olefin) complex has been reported very recently.[32c] (c) Clark, G. R.; Mazid, M. A.; Russel, D. R.; Clark, P. W.; Jones, A. J. *J. Organomet. Chem.* **1979**, *166*, 109.
(33) We keep a local pseudo C_{3v} symmetry around the carbon atoms in the coordinated ethylene. The dotted line drawn in **1** is the corresponding local C_3 axis. In the coordinated alkyl there is local tetrahedral symmetry around the carbon atoms.
(34) Sirvetz, M. H.; Weston, R. E., Jr. *J. Chem. Phys.* **1953**, *21*, 898.
(35) Bénard, M.; Dedieu, A.; Demuynck, J.; Rohmer, M.-M.; Strich, A.; Veillard, A. "Asterix: a system or programs for the Univac 1110", unpublished work. Bénard, M. *J. Chim. Phys.* **1976**, *73*, 413.
(36) Demuynck, J.; Dedieu, A., unpublished results.
(37) Roos, B.; Siegbahn, P. *Theor. Chim. Acta* **1970**, *17*, 209
(38) Whitman, D. R.; Hornback, C. H. *J. Chem. Phys.* **1969**, *51*, 398.
(39) Huzinaga, S. *J. Chem. Phys.* **1965**, *42*, 1293.

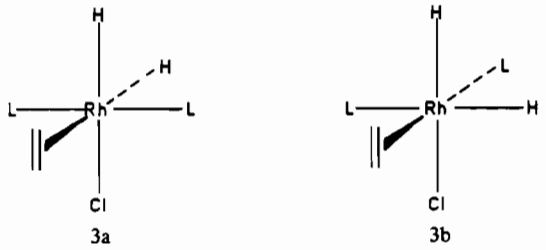

termediate $H_2RhClL_2(C_2H_4)$ were found to be the best candidates for the catalytic cycle. Although **3b** was computed to be slightly more stable (by 2.3 kcal/mol), we pointed out[1] that **3a** is to be preferred, mainly on steric grounds,[40] for the actual PPh_3 ligand. Three different pathways for the hydrogen transfer in **3a** were delineated (they are illustrated in the Scheme I[42]), leading to three stereoisomers of the hydridoalkyl intermediate $HRhClL_2(C_2H_5)$. On the basis of the relative stabilities of these stereoisomers we may tentatively discard the hydrogen migration pathway (moreover the process is computed to be endothermic). The two other pathways—olefin insertion or transfer together with a rearrangement in the reaction plane—seem attractive since they are both computed to be exothermic and lead to the most stable stereoisomers of $HRhClL_2(alkyl)$.[1] **4a** and **4b** are too close in energy, however, to decide, on the basis of their relative energy only, which pathway is to be preferred. Clearly the determination of the reaction path—or at least of some energy profiles—is needed.

The determination of the potential energy hypersurface function of all degrees of freedom—the most important ones are shown in Figure 1—is out of range at the ab initio level. Nevertheless specific questions about the process can be reasonably answered with the aid of two-dimensional cross sections of this hypersurface, and we shall therefore consider such surfaces. We do not allow, to a first approximation, any relaxation of the nonreacting ligands during the transfer process (i.e., we keep θ and ϕ set to zero together with the phosphine ligands along the x axis). Exploratory extended Hückel calculations have indicated that a fairly good picture of the early stage of the process could be given by decreasing the angle between the Rh–H bond and the "Rh–C_2H_4" bond[43] while the C–C bond length of the ethylene was allowed to relax.

The decrease of this angle may result from an increase in either the α angle or the β angle (this would correspond respectively to a hydride migration or to an olefin insertion). Another possibility is an increase of both angles. The SCF potential energy surface function of these two angles—the C–C bond being kept at 1.38 Å—indicates (Figure 2) that the easiest motion is the olefin insertion along the β axis, α being equal or nearly equal to zero.[44] We also note that the ethylene ligand is tilted up by about 15° in its equilibrium position. In addition to the decrease of steric repulsion between the chlorine atom and the ethylene ligand, these features may be explained through the changes occurring in two molecular orbitals of the system. The HOMO (**5**) of the $H_2RhClL_2(C_2H_4)$ system

Scheme I

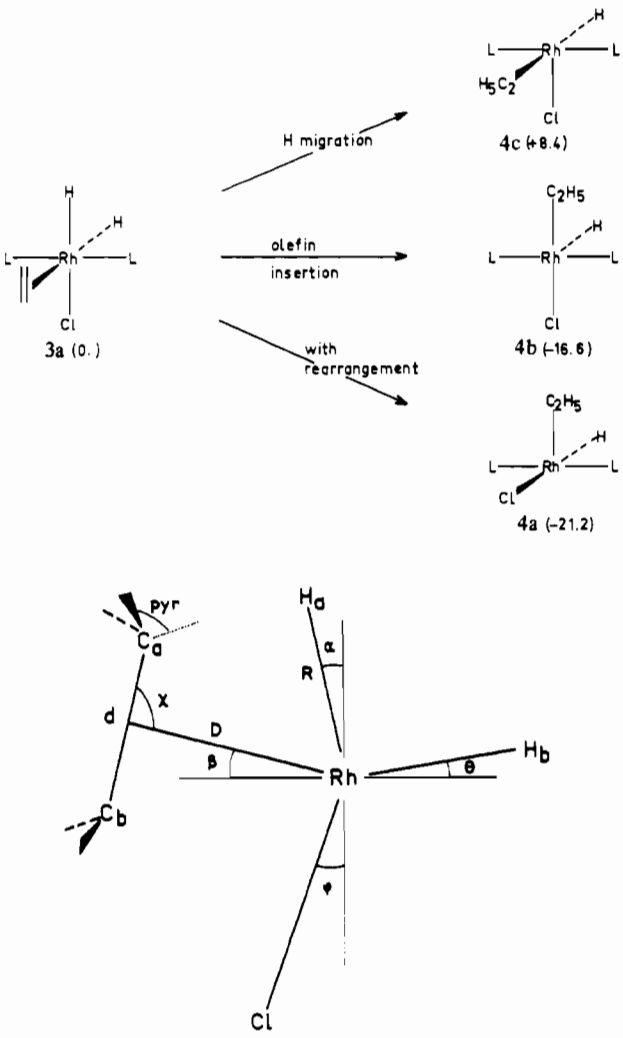

Figure 1. Geometric parameters to be taken into account for the determination of the reaction path.

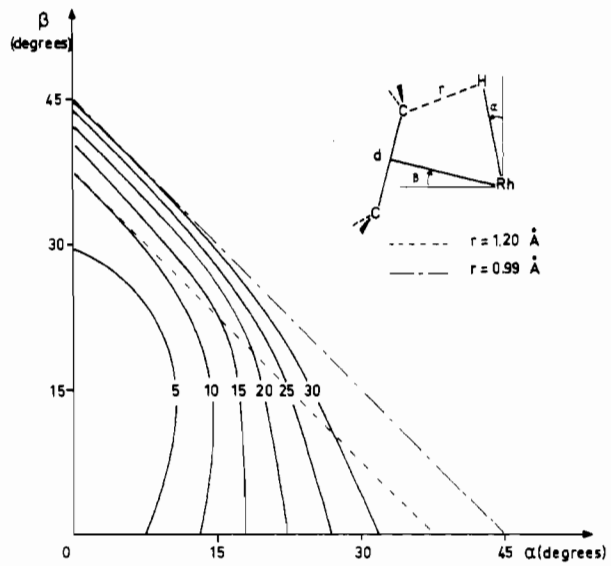

Figure 2. Potential energy surface as a function of the α and β angle. d is kept at 1.38 Å, the zero of energy is for $\alpha = 0$ and $\beta = 15°$, and relative energies are in kcal/mol.

consists mainly of the antibonding combination between the π orbital of the ethylene ligand and a p donor orbital of the chlorine ligand. When either α (**5** → **6**) or β (**5** → **7**) is

(40) PH_3 and PPh_3 have ligand cone angles which are 87 and 145°, respectively.[41]
(41) Tolman, C. A. *Chem. Rev.* **1977**, *77*, 313.
(42) In this scheme and in the following the energies are calculated (in kcal/mol) relative to the **3a** system with the ethylene ligand tilted up by 15°. This tilting lowers the energy of **3a** by 1.9 kcal/mol. In the hydrido-alkyl intermediates the alkyl ligand has the eclipsed geometry. The C–C bond eclipses the Rh–H bond in **4a** and **4b** staggers the Rh–Cl bond in **4c**. It is implicitly assumed that the transferred hydrogen atom is in the plane of the coordinated olefin[13,25] and cis to it.
(43) We refer here to the line from the Rh atom to the center of the ethylene.
(44) The same result is obtained with a C–C bond length of 1.46 Å.

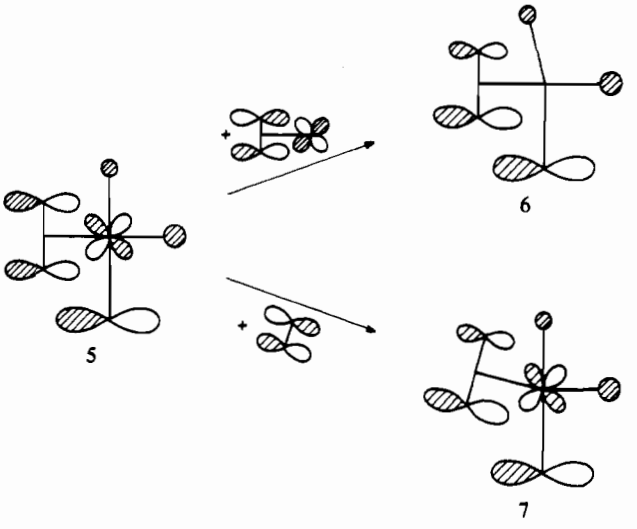

increased, the mixing of the π^* orbital of ethylene polarizes the C_2H_4 π component. The net effect is an increase of the repulsive interaction between $\pi_{C_2H_4}$ and p_{Cl} which is partially relieved, however, in **7** when the ethylene moves upward. An orbital of lower energy **8** is the bonding combination between

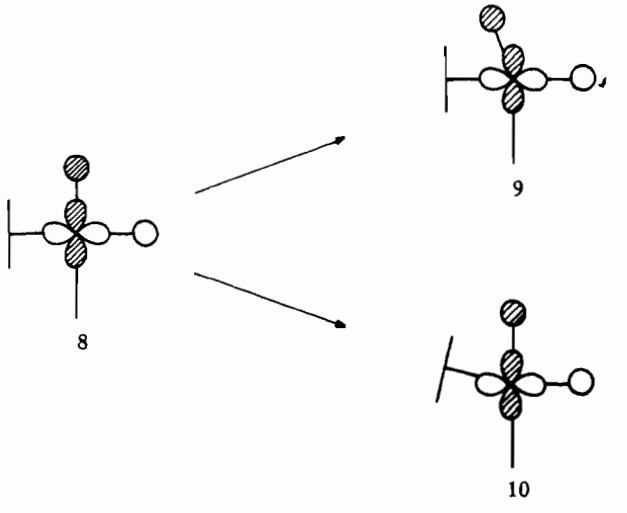

the rhodium $d_{z^2-y^2}$ and the hydride s orbitals. Some of the bonding is lost in **9** when the hydride migrates—in contrast to the olefin insertion **10**—and this adds to the destabilization.

Since the hydride ligand does not depart from its position during the beginning of the ethylene insertion, a reasonable picture of this process will be provided by a surface coupling the ethylene angle β and the C–C bond length variations. The corresponding SCF surface is given in Figure 3. As expected from the mixing of the π^* orbital, the C–C bond length increases with β. The evolution of the bond overlap populations (Table I) for points along the reaction valley is indicative of the progress of the insertion: there is an increase in the Rh–C_b overlap population and a concomitant decrease in the Rh–C_a and Rh–H_a overlap populations which anticipate the formation of the Rh–C_b bond and the breaking of the R–C_a and Rh–H_a bonds. But more intersting is the moderate destabilization (12.8 kcal/mol) of the system for a β angle of 40° and a C–C bond length of 1.54 Å (structure **11**). Note that this point (circled on the surface) corresponds to a C_a–H_a bond length of 1.10 Å (i.e., the equilibrium distance in the alkyl ligand). Furthermore, setting the pyramidality of the hydrogen atoms around the carbon atoms at 109° 28′ reduces the destabilization to 9.5 kcal/mol.

This moderate destabilization can be explained through the simplified interaction diagram[45] (Figure 4) between the

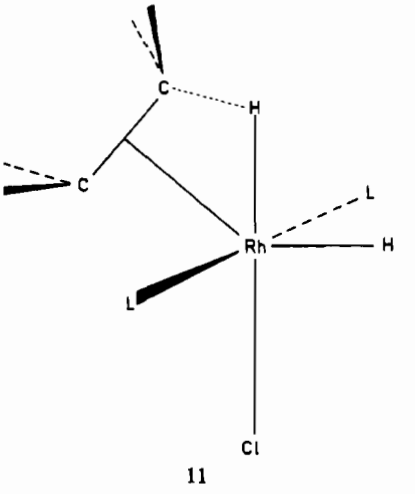

11

$H_2RhCl(PH_3)_2$ fragment and a stretched C_2H_4 fragment. Focusing only on the main interactions, we find two four-electron interactions which should be destabilizing. The first one, between the ethylene π orbital and the s_{H_a} orbital (which is in fact the bonding combination of s_{H_a} and $d_{z^2-y^2}$), is relieved, however, through the mixing with the empty ethylene π^* orbital and with the unoccupied 2a′ and 3a′ orbitals of the $H_2RhCl(PH_3)_2$ fragment[46] (from our calculations 2a′ and 3a′ can be described as $4d_{z^2-x^2}$ and $4d_{x^2-y^2}$ rhodium orbitals, respectively). The same interaction has been previously found in the case of olefin insertion into a Pt–H bond.[23,25] The mixing of the π^* leads to some Rh–C bonding in the upper combination (eq 3) and to some C–H bonding in the lower com-

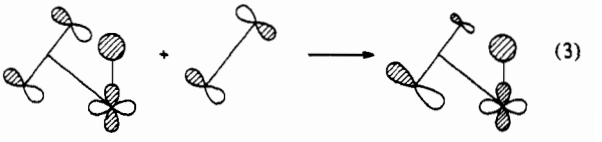

(3)

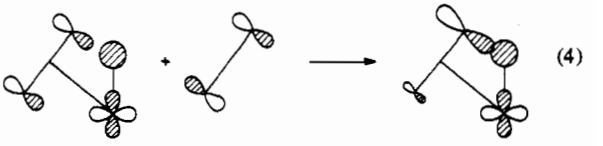

(4)

bination (eq 4).[23,25,47] A second four-electron destabilizing interaction is found between 1a′ (which is the $4d_{yz}$ rhodium orbital) and $3\sigma_g$. Again the associated repulsion is somewhat relieved through the interaction with the unoccupied 2a′ orbital.

We have already pointed out that in **11** the C_a–H_a bond length was 1.10 Å, i.e., the equilibrium distance in the ethyl ligand. Also the C_b–C_a–H_a angle—which amounts to 116.85°—is rather close to the tetrahedral value expected for a $C_2H_5^-$ ligand. This merely results from our starting geometry **1**, in which the Rh–H bond and the Rh–C bond were set at 1.65 and 2.15 Å, respectively[48] (values which are quite typical

(45) In this diagram, qualitatively derived from the SCF valence orbitals of the C_2H_4, $H_2RhCl(PH_3)_2$, and $H_2RhCl(PH_3)_2(C_2H_4)$ systems, only orbitals of A′ symmetry (with respect to the migration symmetry plane) have been drawn. For the sake of simplicity the orbitals of the H_b, Cl, and PH_3 ligands have been discarded although they give some contributions to the drawn orbitals (see, for instance, the HOMO **5**).

(46) The situation is in fact somwhat more complicate because of some additional mixing of the antibonding combination of the p Cl orbital and 1a′ (see **5**).

(47) Pearson, R. G. "Symmetry Rule for Chemical Reactions"; Wiley-Interscience: New York, 1976.

(48) The C–C–H angle would be even closer to 109° 28′ for a shorter metal–hydrogen bond.[49]

(49) Recent evaluations of the Rh(III)–H bond seem to indicate that it is rather short.[50,51]

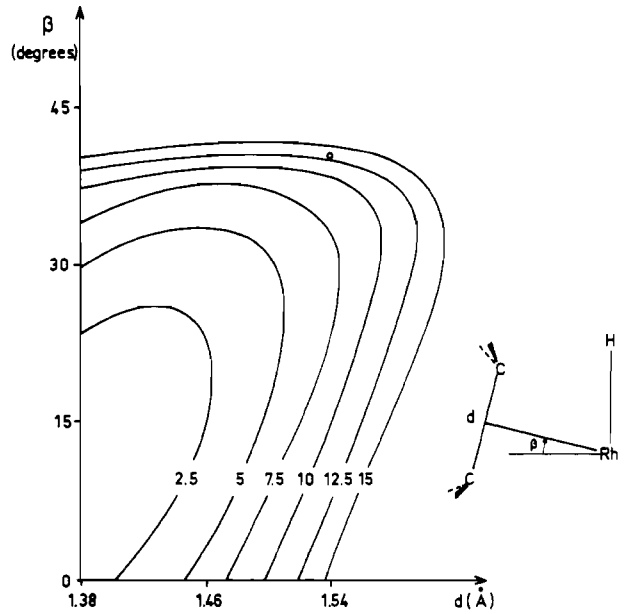

Figure 3. Potential energy surface for the early stage of the insertion process. α is kept at 0, the zero of energy is for d = 1.38 Å and β = 15°, and relative energies are in kcal/mol.

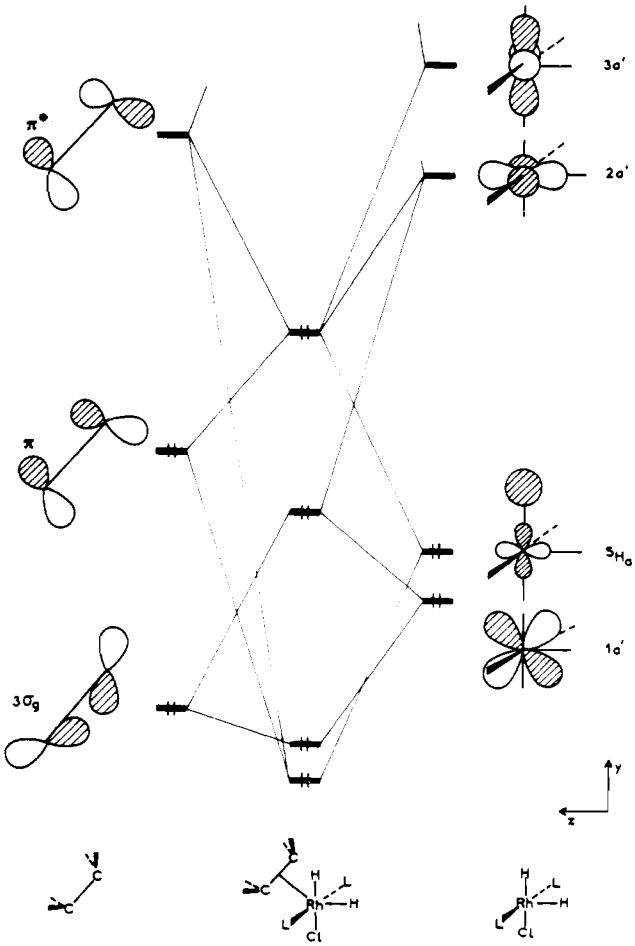

Figure 4. Simplified interaction diagram for $H_2RhCl(PH_3)_2$ and the stretched C_2H_4 fragment to compose **11**. Only selected orbitals of the insertion plane are shown.

for metal hydrogen and metal C(sp^2) bonds). We note that the same angle of 50° between the Rh–H bond and Rh–C_2H_4

(50) Yoshida, T.; Thorn, D. L.; Okano, T.; Ibers, J. A.; Otsuka, S. *J. Am. Chem. Soc.* **1979**, *101*, 4212 and references therein.

Table I. Bond Overlap Population during the Approach of C_2H_4

	$\beta = 0°$, $d = 1.38$ Å	$\beta = 15°$, $d = 1.38$ Å	$\beta = 30°$, $d = 1.46$ Å	$\beta = 40°$, $d = 1.54$ Å	$\beta = 40°$, $d = 1.54$ Å, pyr = 109° 28′
Rh–H_a	+0.32	+0.29	+0.20	+0.13	+0.11
Rh–H_b	+0.31	+0.29	+0.27	+0.27	+0.28
Rh–C_a	+0.07	+0.08	+0.04	+0.01	+0.01
Rh–C_b	+0.09	+0.08	+0.10	+0.13	+0.15
C_a–H_a	+0.03	+0.09	+0.27	+0.43	+0.50

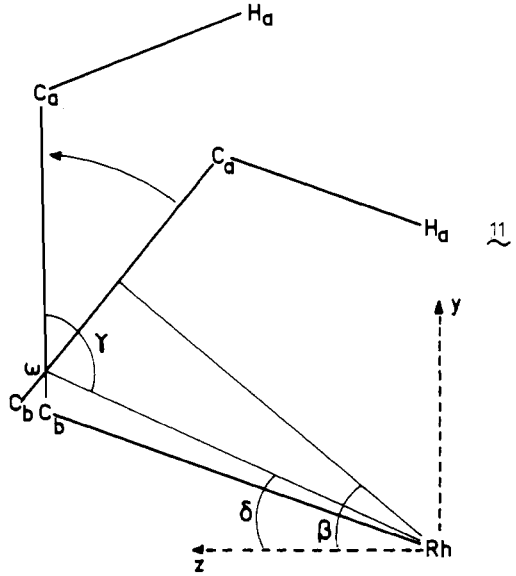

Figure 5. Unrelaxed (**11**) and relaxed geometries of the alkyl ligand in the hydrido–alkyl intermediate.

bond has been found (through extended Hückel calculations) for the transition state in the ethylene insertion into the Pt–H bond of the *cis*-$HPt(PH_3)_2$(ethylene)$^+$ system.[25] There are also electronic similarities between the (C_2H_4 + H_a) entity and the free $C_2H_5^-$ system since the molecular orbitals of **11** which are mainly of (C_2H_4 + H_a) character look like $C_2H_5^-$ orbitals. The geometry of (C_2H_4 + H_a) in **11** can thus be viewed as an unrelaxed geometry of the ethyl ligand (with a Rh–C_b bond length of 2.18 Å and a RhC_bC_a angle of 69° 18′) in opposition to the relaxed geometry [which would correspond to Rh–C_b = 2.05 Å and RhC_bC_a = 109° 28′ (see **2**)].

We also investigated the relaxation of the nonreacting ligands for this geometry. Increasing either the θ or the ϕ angles from 0 to 45° led to an overall destabilization of the system.[52] This supports our previous assumption that the potential energy surface shown in Figure 3 is a fairly good representation of the many dimensional surface for the beginning of the reaction.

Is **11** the transition state for the insertion process? To answer this question we have to go further and to consider the relaxation of the alkyl ligand from its unrelaxed geometry in **11**. This process is shown schematically in Figure 5. We allow the variation of the Rh–C_b bond length and of the RhC_bC_a bond angle with an additional degree of freedom for the ethylene rotation angle β.[53] In order to compute a two-

(51) Cowie, M.; Dwight, S. K. *Inorg. Chem.* **1979**, *18*, 1209.

(52) For an intermediate angle of 22.5° the destabilization amounts of 9.4 kcal/mol and to 9.5 kcal/mol when rotating the Rh–H_b bond and Rh–Cl bond, respectively.

(53) A fixed value of 109° 28′ has been assumed for the $C_bC_aH_a$ angle throughout the alkyl relaxation process. This contributes an additional 8.6 kcal/mol to the destabilization of **11**. This extra destabilization is particular to **11** since it may be traced to the resulting Rh–H_a bond length (1.51 Å) being too short (in $H_2RhCl(PH_3)_2$ the optimized SCF Rh–H bond length is 1.57 Å[2]). This constraint is relieved when the RhC_bC_a angles increase.

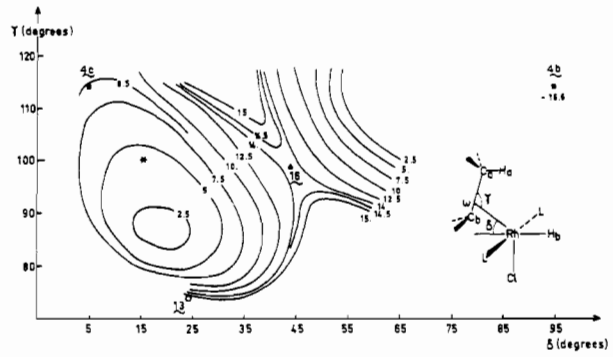

Figure 6. Potential energy surface for the relaxation of the alkyl ligand as a function of the δ and γ angles only. No relaxation of Cl and H_b is allowed. The zero of energy is the same as in Figures 2 and 3 ($\alpha = 0$, $\beta = 15°$).

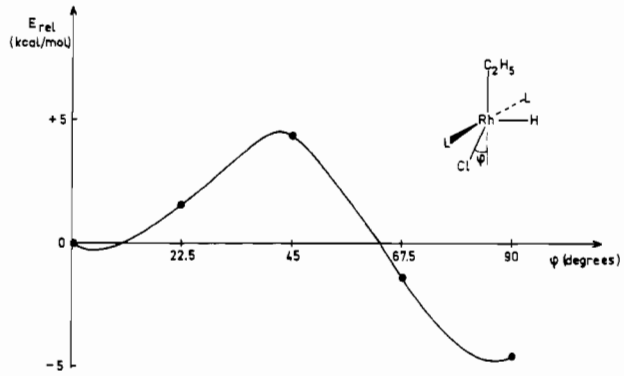

Figure 7. Potential energy curve for the chlorine rotational motion around the $[HRhL_2(C_2H_5)]^+$ pseudo-C_{2v} fragment. The energy zero refers to structure **4b**.

dimensional surface only, we have reduced these three parameters to the two parameters γ and δ as defined in Figure 5. γ goes from 74° (in **11**) to 114° (corresponding to RhC_bC_a = 109° 28′), and δ varies between 4.7° (Rh–C_b collinear to the z axis) and 94.7° (Rh–C_b collinear to the y axis). The corresponding SCF surface $E = f(\gamma,\delta)$ is shown in Figure 6.

Starting from **11** there are two channels on this surface corresponding either to an increase or to a decrease in the δ angle and leading to the **4b** or the **4c** stereoisomers of the $HRhClL_2$(alkyl) intermediate, respectively. The channel leading to the **4b** structure (with H in apical position) is characterized by a transition state, the geometry of which is shown in **12**. The whole process is exothermic by about 16.6

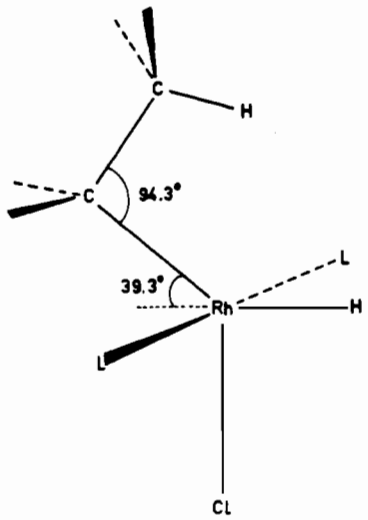

12

kcal/mol, and the energy barrier is computed to be 14.1 kcal/mol. The origin of this barrier is traced to the HOMO **13** which consists mainly of the antibonding combination

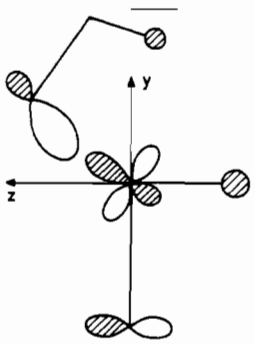

13

between the lone pair of a distorted ethyl ligand and the occupied d_{yz} orbital of the $[HRhClL_2]^+$ fragment. The barrier is moderate, however, due to the stabilization of this antibonding combination by the empty d levels of the $[HRhClL_2]^+$ fragment. If δ is increased further, the lone pair of the alkyl ligand moves toward the nodal plane of the rhodium d_{yz} orbital, the repulsive interaction is relieved, and one gets a net stabilization. The channel leading to **4c** is characterized by a secondary minimum. This again results from a decreased antibonding interaction between the rhodium d_{yz} and the lone pair of the ethyl ligand. The energy of the system then goes up since one gets a very unstable stereoisomer (**4c**) of the $HRhClL_2(C_2H_5)$ system (this was traced to the Cl atom in apical position[1]). The surface also tells us that **4c** is not a true intermediate.

These results would therefore suggest that **4b** is the stereochemistry of the hydridoalkyl intermediate in the catalytic cycle. But we have to remember that **4b** is not the most stable $HRhClL_2(C_2H_5)$ isomer [**4a** is more stable by 4.6 kcal/mol (see Scheme I)] and that the relaxation of the other ligands, the in-plane[54] Cl and H_b ligands as well as the two out-of-plane[54] phosphine ligands, has not been allowed yet. Rearrangements of nonreacting ligands have been found to be important for the olefin insertion into a Pt–H bond[25] (where the metal has formally a d^8 configuration). However they seem to play no role in the case of the methyl migration reaction in the $CH_3Mn(CO)_5$ system[55] (where the metal has formally a d^6 configuration). Another problem is whether they would occur during or after the insertion process.

We first investigated the possibility of ligand rearrangements in **4b** and **4c**. One way of going from **4b** to **4a** is to rotate the Rh–Cl bond as shown in Figure 7. This is an easy process since it requires only 4.5 kcal/mol to go through the pseudo-C_{2v} geometry corresponding to $\varphi = 45°$. Another process would be the inverse of a Berry pseudorotation going through a TBP complex with Cl, H_b, and C_2H_5 in the equatorial plane. From our previous calculations the TBP geometry is higher in energy by at least 12 kcal/mol than the pseudo-C_{2v} geometry.[56] The

(54) We refer here to the insertion plane.

(55) Berke, H.; Hoffmann, R. *J. Am. Chem. Soc.* **1978**, *100*, 7224.

(56) For a staggered geometry of the alkyl ligand the TBP geometry is computed to be 12 kcal/mol higher in energy than the pseudo C_{2v} geometry with an eclipsed alkyl ligand.[1] Rotating by 180° the end-on methyl group of the alkyl ligand in the TBP geometry, where there are no steric contacts from the other ligand, would destabilize this geometry by about 2 kcal/mol.[57]

(57) In the **4a** geometry the methyl rotation barrier in the coordinated alkyl ligand has been computed to be 1.6 kcal/mol.

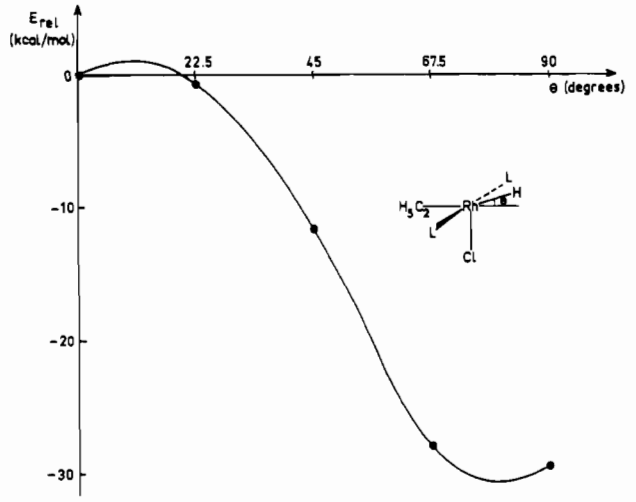

Figure 8. Potential energy curve for the hydrogen rotational motion around the $[ClRhL_2(C_2H_5)]^+$ pseudo-C_{2v} fragment. The energy zero refers to structure **4c**.

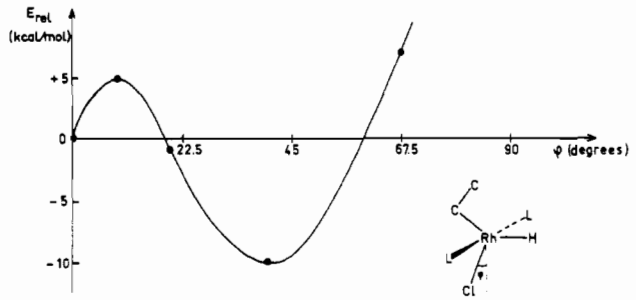

Figure 9. Potential energy curve for the chlorine rotational motion starting from structure **12**.

moderate destabilization of the pseudo-C_{2v} geometry is traced to a favorable interaction **14** between the π-donor orbital of

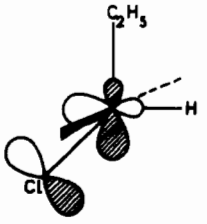

14

the chlorine ligand and an empty orbital of b_2 symmetry of the $[HRh(PH_3)_2(C_2H_5)]^+$ fragment.[58]

The rotation of the Rh–H bond in the **4c** geometry would lead to the **4a** structure. The energetics of the process is shown in Figure 8. The great exothermicity and the quasi-absence of an energy barrier reflect the great tendency of the Cl ligand to be in a basal position.

The ease of these rearrangement processes either from **4b** or from **4c** suggest that they are probably occurring *during* the alkyl relaxation process. This has been checked by looking at the chlorine rotational motion for **12** and at the hydrogen rotational motion for one intermediate point (corresponding to $\delta = 15°$ and $\gamma = 100°$, starred on the surface). In both cases (see Figures 9 and 10) some angular relaxation is achieved, the stabilization being of the order of 10 kcal/mol. We note that in both cases the resulting structures again reflect the tendency of this system for a square-pyramid geometry with the alkyl ligand in apical position. In fact the distinction

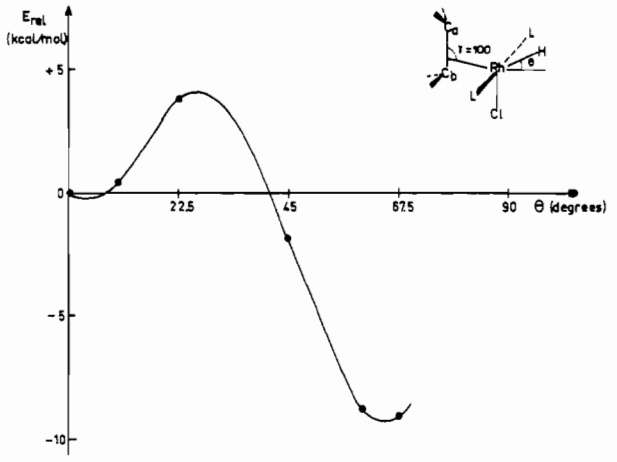

Figure 10. Potential energy curve for the hydrogen rotational motion starting from the structure corresponding to $\delta = 15°$ and $\gamma = 100°$.

between the two channels, once the in-plane ligands are allowed to relax, is rather formal. The most rigorous way to cope with this relaxation problem would be to compute the tridimensional surface function of the γ, ω–Rh–Cl, and ω–Rh–H_b angles, but this is out of range at the SCF level (it would require at least 10^3 distinct calculations). Nevertheless we can rather safely conclude that in-plane rearrangements[59] during the alkyl relaxation process do occur, leading to an overall stabilization of the system. This result leads to two other important conclusions: (i) **4a** is probably the geometry of the hydrido–alkyl intermediate in the catalytic cycle; (ii) **11** can be considered as a good representation of the transition state for the whole insertion process.

Discussion

Energetic and Geometric Features of the Insertion. The computed exothermicity of the reaction is about 17 kcal/mol. For the energy transfer barrier we calculate an upper limit[53] of 18 kcal/mol. From experimental studies it has been concluded that the hydrido–alkyl intermediate formation was a reversible reaction for trisubstituted cycloalkenes[5] but could be considered as being irreversible[60] (near room temperature) in the case of less highly substituted alkenes.[5,61] Experimental activation energies for the hydrogenation of cyclohexene in benzene range between 7 and 19 kcal/mol.[3c,62,63] In a related process, the insertion of C_2H_4 into the Rh(III)–C_2H_5 bond of a six-coordinate intermediate involved in an ethylene dimerization reaction,[64], the activation energy amounts to 17 kcal/mol. The SCF results are therefore in reasonable agreement with the known experimental data.[65]

One may of course question the validity of the present results especially with regard to the quality of the basis set and the correlation energy error. The comparison with theoretical studies of the uncatalyzed reaction $H^- + C_2H_4 \rightarrow C_2H_5^-$ is

(58) Lichtenberger, D. L.; Brown, T. L. *J. Am. Chem. Soc.* **1978**, *100*, 366.

(59) In the structure corresponding to $\delta = 15°$, $\gamma = 100°$, and $\theta = 67.5°$, bending of the two Rh–P bonds out the x axis toward a pseudo C_{4v} geometry resulted in a destabilization of 4.8 kcal/mol for a P–Rh–P angle of 160°. This suggests that out-of-plane rearrangements are probably not important in the relaxation process.

(60) This might well arise from a much greater alkane reductive elimination rate in the next step compared to the rate for the reverse reaction of the olefin insertion.[5,61]

(61) Biellmann, J. F.; Jung, M. J. *J. Am. Chem. Soc.* **1968**, *90*, 1673.

(62) Demortier, Y.; de Aguirre, I. *Bull. Chem. Soc. Chim. Fr.* **1974**, 1619.

(63) Rousseau, C.; Evrard, M.; Petit, F. *J. Mol. Cat.* **1977**, *3*, 309.

(64) Cramer, R. *J. Am. Chem. Soc.* **1965**, *88*, 4717.

(65) We are well aware of the fact that the RhCl(PPh$_3$) catalyst is almost inactive for the hydrogenation of C_2H_4.[3] This has been traced to the formation of a relatively stable $RhCl(PPh_3)_2(C_2H_4)$ complex which cannot activate H_2[3c]. This does not preclude however, the existence of the ethylene insertion into a Rh(III)–H bond (see for instance ref 21).

instructive in this respect. The exothermicity for this reaction has been computed to be 3.3 kcal/mol[66] both at the SCF and at the CEPA level (where electron correlation is introduced) with an extended basis set.[67] Another calculation[68] using a standard 4-31G[69] basis set (which is, like ours, of double-ζ quality for the valence shells) gives an exothermicity of −20.7 kcal/mol. Such a high value is probably due to an unbalanced respresentation of the wavefunctions of H^-, C_2H_4, and $C_2H_5^-$.[70] Improving the description of the wavefunctions with a 3 × 3 configuration interaction calculation leads to a much smaller value (−2.0 kcal/mol). The energy barrier follows the inverse trend: +1.9 kcal/mol with the 4-31G basis set; +16.6 kcal/mol for the 4-31G + CI 3 × 3 calculation. From these results, one might think that our calculated values for the exothermicity and for the barrier of the hydrogen-transfer step are overestimated and underestimated, respectively. In our case however, the H_a ligand is far from being a pure H^- anion,[71] and we may expect that the basis set used in this study gives a more uniform description of the H_a, C_2H_4, and C_2H_5 ligands. As far as the electron correlation error is concerned, we already mentioned that the same value was obtained for the exothermicity of the $H^- + C_2H_4 \rightarrow C_2H_5^-$ reaction both at the SCF and the CEPA levels. Since in the insertion-type reactions the number of bonds remains constant, the correlation energy may be expected to be approximately constant[29b] along the reaction path.

The reaction is best described as an insertion reaction. This motion, as we have shown, is induced by the repulsive interaction between the olefin π orbital and the Cl p orbital. A similar repulsive interaction would be found for any σ- or π-donor ligand substituting the chlorine ligand cis to the olefin. The only hydrido–alkyl intermediate characterized so far[16] has the stereochemistry shown in **15**. This stereochemistry is

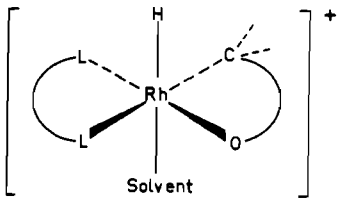

15

consistent only with an insertion of the olefin into the Rh–H bond from **16**, the parent dihydrido olefinic intermediate.[72]

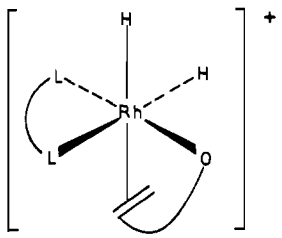

16

In **16** the ligand cis to the olefin (in the insertion plane) is a phosphine ligand which is a moderate σ donor. On the other hand, a complex with a π-acceptor ligand cis to the olefin should be less prone to undertake the insertion motion.

We have also shown that an in-plane rearrangement is likely to occur in the H_2RhClL_2(olefin) system during the insertion process. This is apparently not the case for the olefin insertion in **16**. The situation is not quite analogous however: there is no in-plane π-donor ligand in **16** (like Cl in **3a**), and we have previously stressed the importance of such a ligand for the in-plane rearrangement.

Substitution Effects. How would the insertion process be perturbed by substituting the chlorine atom, the phosphine ligands, or the olefin itself? The analysis will be focused on the interaction diagram (Figure 4) for the transition state **11** and more precisely on the two repulsive interactions which are the main contributors to the activation energy.[73,74] But before going into the details of the discussion, one must realize that our conclusions will strictly refer to the insertion and not to the whole hydrogenation reaction. The hydrogenation reaction is a multistep process, and some factors which favor the insertion reaction might for instance hinder the previous steps in the catalytic cycle.[75]

We first discuss the substitution of the chlorine atom. We have already pointed out that the π-donor character of Cl was of some importance for the rotational motion of the olefin and for the in-plane rearrangements during the insertion. We now look at the effect on the energy barrier. The ligand X in H_2RhXL_2(olefin) will mostly act through its π-interacting capability with the 1a′ orbital. Compared to Cl a better π donor would raise the 1a′ level. Because of a greater energy difference between the 1a′ and $3\sigma_g$ levels, the repulsive interaction between those two levels should be decreased and the activation energy should be lowered accordingly. The opposite would hold for a π acceptor. $RhBr(PPh_3)_3$ and $Rh(SnCl_3)(PPh)_3)_3$ are known to be more active[76] and less active,[3c] respectively, than $RhCl(PPh_3)_3$. This corroborates our analysis[77] although the difference in the stability constants of the corresponding dihydrido olefinic intermediates also plays a role.[80] We also note that in the ethylene dimerization reaction,[63] which we mentioned previously, the necessity for halides (probably as ligands of the six-coordinate hydrido olefinic intermediates) has been stressed.

The perturbation created by the ligand substitution at the metal may as well arise from the ability of the substituents to alter the formal charge of the metal center. The substitution of the phosphine ligands provides an example of this effect. Since these ligands are off the migration plane, their σ and π orbitals do not interact with the orbitals which control the activation energy, and their substitution should not affect it.

(66) Kollmar, H. *J. Am. Chem. Soc.* **1978**, *100*, 2665.
(67) This is a (7,3/3) basis set[39] contracted to 4,2/2, i.e., of double-ζ type, with added d polarization functions on the carbon atom and diffuse s and p functions on the carbon and hydrogen atoms.
(68) Strozier, R. W.; Caramella, P.; Houk, K. N. *J. Am. Chem. Soc.* **1979**, *101*, 1340.
(69) Ditchfield, R.; Hehre, W. J.; Pople, J. A. *J. Chem. Phys.* **1971**, *54*, 724.
(70) The energy obtained for H^- with this basis set is too high in comparison with the energy obtained for C_2H_4 and $C_2H_5^-$.
(71) The charge of the H_a ligand in the **3a** system (given by the population analysis) is −0.168 e.
(72) Since in **15** the alkyl ligand and the second hydride ligand are coplanar, both hydrides and the olefin must be coplanar in the dihydrido olefinic intermediate. There is only one structure **16** satisfying this condition together with the additional requirements of the cis disposition of the two hydride ligands (since the oxidative addition of H_2 is likely to be cis) and of the chelating diphsophine ligand.
(73) We have made the simplifying assumption that the reaction paths for the substituted system and the $H_2RhCl(PH_3)_2(C_2H_4)$ system were identical.
(74) A more rigorous presentation would take into account the effect of the perturbation on the dihydrido olefinic intermediate too. The analysis of the wavefunctions of both the dihydrido olefinic complex **3a** and the transition state **11** indicates however that the interactions between the $(H_2RhClL_2)^+$ and the C_2H_4 fragments are rather weak in **3a** compared to those in **11**.
(75) Harmon, R. E.; Gupta, S. K.; Brown, D. J. *Chem. Rev.* **1973**, *73*, 21.
(76) Jardine, F. H.; Osborn, J. A.; Wilkinson, G. *J. Chem. Soc. A* **1967**, 1574.
(77) It is implicitly assumed that Br^- is a better π donor than Cl^-. Although this is in agreement with the ordering of π-orbital energies, the difference in the π-donor abilities could be offset by a greater π overlap—between the halogen p orbital and the corresponding metal d orbital—Cl^- compared to Br^-.[78,79] This would not change our conclusion however: because of a greater mixing, the 1a′ level would have less metal character for $RhBr(PPh_3)_3$ than for $RhCl(PPh_3)_3$ and would therefore interact less with the $3\sigma_g$ level.
(78) McKinney, R. J.; Pensak, D. A. *Inorg. Chem.* **1979**, *18*, 3413.
(79) Hall, M. B. *J. Am. Chem. Soc.* **1975**, *97*, 2057.
(80) Rousseau, C.; Evrard, M.; Petit, F. *J. Mol. Cat.* **1979**, *5*, 163.

But a more electron-withdrawing ligand would increase the formal positive charge of the rhodium atom. The 1a′ level would be lowered; hence the repulsive interaction with the $3\sigma_g$ level would be strengthened and the energy barrier greater. An electron-releasing ligand would behave exactly in the opposite way. Experimentally the activity of the $RClL_3$ catalyst is decreased for electron acceptors substituted on the aromatic nuclei and increased for electron donors[81-83] (it has also been pointed out that a greater equilibrium constant in the H_2 oxidative addition arising from a decrease in the formal positive charge of the metal would give some contribution to the hydrogenation rate enhancement[81]).

We now turn our attention to the substitution of the ethylene substrate and see how it will modify the three C_2H_4 orbitals. We know that the barrier should be lowered when the two four-electron repulsive interactions are minimized through either a greater energy difference and/or a smaller overlap between the interacting levels $3\sigma_g/1a'$ and π/s_{H_a}. A contribution to the stabilization of the transition state is also expected when the π^* orbital has a lower energy and/or a greater overlap with the s_{H_a} orbital. Since the overlap between s_{H_a} and either π or π^* is highly directional (mostly between C_a and H_a), the polarization of the π and π^* orbitals upon the substitution[84] is expected to have some influence on the energy barrier and on the directionality of the insertion when the olefin is unsymmetrically substituted (the regioselectivity in olefin insertion has been reviewed recently.[12]) We shall successively study three representative examples of olefins, the propylene, the acrylonitrile, and the styrene molecules.

The polarization of the π and π^* orbitals induced by the methyl substituent in the propylene molecule[85] is shown in **17** and **18**, respectively. The same polarization would be obtained

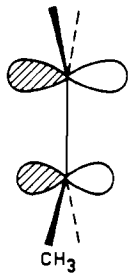

17

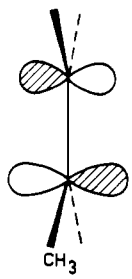

18

for higher 1-olefins $RCH{=}CH_2$. For such a dissymmetric olefin we can think of two isomers for the dihydrido olefinic intermediate $H_2RhClL_2(RCH{=}CH_2)$ either **19** or **20**. The

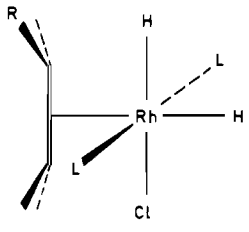

19

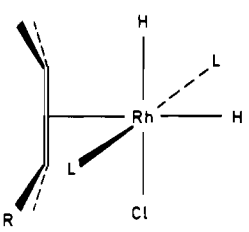

20

repulsion between the polarized π orbital and the Cl p orbital [which we have already seen in the context of the olefin rotation (see 7)] is minimized in **20** but not the steric repulsion between R and Cl which would be less important in **19**. If we now proceed along the insertion reaction path up to the transition state, we expect the insertion from **19** to be favored over the insertion from **20** and hence the hydrogen atom to add on the carbon atom α to R. The rationale behind this statement lies in the difference in the $\langle\pi|s_{H_a}\rangle$ and $\langle\pi^*|s_{H_a}\rangle$ overlaps: starting from **19** minimizes the overlap between π and s_{H_a} (see **21**) and maximizes the overlap between π^* and

21

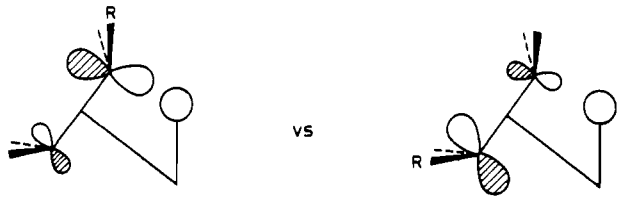

22

s_{H_a} (see **22**). Both factors therefore contribute to a reduced repulsive interaction between these two levels. Extended Hückel calculations carried out for the two corresponding transition-state geometries[73] indeed show this effect in the π/s_{H_a} interaction. The total energies, however, follow the reverse trend. Whether or not this is due to an artefact in the extended Hückel calculations, to some other subtle interactions,[86] or to the lack of geometry optimization,[73] the difference is too small (2.3 kcal/mol) to be conclusive. We note that experimentally the first hydrogen atom has been found to add primarily α to the substituent when R is a cyclopropyl ring.[87] The absence of isomerization during the hydrogenation of 1-pentene was again traced to the first hydrogen adding α to the propyl substituent.[4]

Both stereochemistries **19** and **20** will of course give the same hydrogenated product if there is no rearrangement in the hydrido–alkyl intermediate before the second hydrogen transfer. If the transfer of the first hydrogen atom is followed by some other reaction, then the final product would be different. In this case **19** and **20** would lead to the linear and branched products, respectively. This problem is important for instance in the hydroformylation process, but the hydridoolefinic intermediate involved is a pentacoordinate d^8 metal complex, and this changes the nature of the problem.

For a comparison of the propylene insertion barrier to the ethylene insertion barrier, both the overlaps and the energies of the interacting orbitals must be considered. The overlap factor favors the propylene since the π/s_{H_a} repulsive interaction is reduced. The methyl substitution raises both the $3\sigma_g$ and π levels. This is favorable for the π/s_{H_a} interaction but the corresponding stabilizing effect could be offset by an increased repulsion between $3\sigma_g$ and 1a′. No definite conclusion can therefore be given without a more detailed study. Experimentally, methyl substitution in cyclohexene is found to lower

(81) Montelatici, A.; van der Ent, A.; Osborn, J. A.; Wilkinson, G. *J. Chem. Soc. A* **1968**, 1054.
(82) James, B. R. "Homogeneous Hydrogenation"; Wiley: New York 1973; pp 230–233.
(83) Replacement of the phenyl groups by more basic groups decreases the activity of the catalyst, but this has been explained by a reassociation equilibrium leading to an inactive six-coordinate species.
(84) For a theoretical discussion of the polarization phenomena, see: Libit, L.; Hoffmann, R. *J. Am. Chem. Soc.* **1974**, *96*, 1370.
(85) (a) See ref 84 and references therein. (b) See also: Houk, K. N. *J. Am. Chem. Soc.* **1973**, *95*, 4092; *Acc. Chem. Res.* **1975**, *8*, 361.
(86) Some repulsive interaction between s_{H_a} and the nonnegligible component on the α-carbon atom of the $\sigma\pi$ methyl orbital[84] could contribute to a favored insertion from **20**.
(87) Heathcock, C. H.; Poulter, S. R. *Tetrahedron Lett.* **1969**, 2755.

the enthalpy of activation of the whole hydrogenation reaction catalyzed by $RhCl(PPh_3)_3$.[76]

The acrylonitrile case will be discussed more briefly. Since the CN substituent acts mainly as a σ donor and a slight π acceptor, the polarization of the acrylonitrile π system will essentially be the polarization of the π^* orbital induced by second-order mixing of π into π^* via the π-acceptor orbital of CN.[88] The π orbital (which is not drawn) is practically not perturbed. The polarized π^* orbital is sketched in **23**.

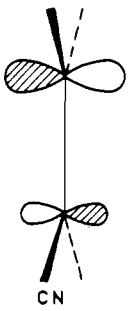

23

Compared to the propylene π^* orbital **18** the polarization occurs in the opposite direction. Our previous conclusions are therefore reversed. **19** should be preferred as the equilibrium geometry of the dihydrido olefinic intermediate since it minimizes the steric repulsion. On the other hand the insertion from **20** should be favored due to a greater stabilizing effect of the π^* orbital. This is in agreement with the formation of (1-cyanoethyl)metal d^6 complexes rather than 2-cyanoethyl complexes in the reaction of some monohydrido d^6 metal complexes with acrylonitrile.[90,91]

In the acrylonitrile case too, the effect on the energy barrier caused by the CN substition in C_2H_4 is difficult to evaluate. The π^* level is lowered (because of the π-acceptor ability of CN), thus stabilizing the π/s_{H_a} interaction. The $3\sigma_g$ level is raised appreciably (CN being a rather strong σ donor), and its repulsive interaction with 1a′ is enhanced. Again one effect could balance the other.

What about the styrene case? Two phenyl π orbitals (which are symmetric with respect to the pseudo mirror plane) will interact rather strongly with the ethyl π system.[92] This is shown in Figure 11. π_S (belonging to the e_{1g} set) interacts with π, π^*_S (belonging to e_{2u}) with π^*. In addition to this first-order mixing, there is also second-order mixing between π and π^* as between π_S and π^*_S. The polarized orbitals are shown in Figure 11. Both $\pi + \pi_S$ and $\pi_S - \pi$ would interact with s_{H_a}. Since they are polarized in the reverse direction,[92] this interaction is not expected to govern the directionality of the insertion.[93] The polarized $\pi^* + \pi^*_S$ orbital has an increased atomic coefficient at the β ethylene carbon atom (like in **23**). This should again favor the insertion from **20**.

Conclusion

We already stressed[1] some limitations of such a theoretical study. Rather than calculating the full energy hypersurface, we have based our reasoning on successive two-dimensional surfaces. Also since we are mainly concerned with a reaction path determination, some possible deficiency of the basis set and the neglect of correlation might alter some of our results. Clearly these effects warrant a separate theoretical study. Nevertheless we think that our main conclusions would not be modified.

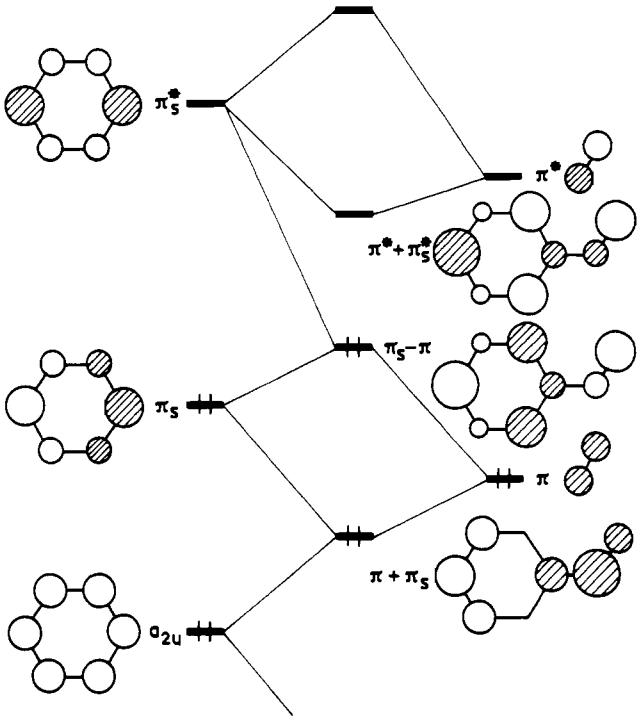

Figure 11. Interaction diagram (based on extended Hückel calculations) for the phenyl fragment with the ethyl fragment. Only selected π orbitals (see the text) are shown.

From these calculations, a good approximation of the reaction path up to the transition state is found by considering the rotational displacement of the olefin simultaneously with the lengthening of the C–C bond. In the transition state the alkyl ligand is not far from its equilibrium geometry. We have shown that the end of the reaction was characterized by concomitant rearrangements of the non reacting ligands. The insertion process is calculated to be exothermic and the energy barrier is moderate, in agreement with experimental data. The metal substitution pattern has been studied. More specifically, we have stressed the importance of a π-donor ligand in the coordination sphere ($RhH(PPh_3)_3$ is known to catalyze the hydrogenation of C_2H_4 but through a different mechanism[95]). Finally an orbital picture has been given for analyzing the directionality of the insertion for olefins other than C_2H_4.

We can go somewhat further than the hydrogenation reaction and think to a more general process, the insertion of an olefin into a d^6 metal–alkyl bond.[64,96] Replacing H by CH_3 or an alkyl ligand would probably not change the main features of the analysis. In the interaction diagram of Figure 4, the alkyl σ-donor orbital would probably be at a higher energy than the s_{H_a} orbital (since the alkyl ligand is a better σ donor). One would therefore expect a greater destabilization interaction with the olefin π orbital and hence a greater barrier. We note that, in some instances, no olefin insertion into a d^6 metal–alkyl bond was observed.[16,97] Clearly the insertion of an olefin into a metal–alkyl bond needs further theoretical study. Another topic of interest would be the alkyne insertion

(88) The coefficient of the β-carbon atom in the HOMO is slightly greater than the coefficient of the α-carbon atom, both in extended Hückel calculations and in SCF calculations performed with our basis set (a larger separation was found from CNDO/2 calculations[89]).
(89) Houk, K. N.; Munchausen, L. L. *J. Am. Chem. Soc.* **1976**, *98*, 937.
(90) Ariyaratne, J. K. P.; Green, M. L. H. *J. Chem. Soc.* **1963**, 2976.
(91) Dewhirst, K. C. *Inorg. Chem.* **1966**, *5*, 319.
(92) From extended Hückel calculations.
(93) Calculations[94] carried out with a minimal basis set (STO-3G) do not show any significant change in the total π atomic charges, most atoms having π-electron population close to zero.
(94) Hehre, W. J.; Radom, L.; Pople, J. A. *J. Am. Chem. Soc.* **1972**, *94*, 1496.
(95) Strauss, S. H.; Shriver, D. F. *Inorg. Chem.* **1978**, *17*, 3069.
(96) Evitt, E. R.; Bergman, R. G. *J. Am. Chem. Soc.* **1979**, *101*, 3973.
(97) Green, M. L. H.; Mahtab, R. *J. Chem. Soc., Dalton Trans.* **1979**, *262*.

reaction. Work along these lines is now in progress.

Acknowledgment. Calculations have been carried out at the Centre de Calcul du CNRS in Strasbourg-Cronenbourg. We thank the staff of the Centre for their cooperation. Some initial calculations on this reaction were done in our group by Dr. A. Rossi. This work has been supported through ATP No. 3790 of the CNRS.

Registry No. 3a, L = PH_3, 72152-08-0; **4a**, L = PH_3, 72152-09-1; **4b**, L = PH_3, 72173-82-1; **4c**, L = PH_3, 72173-87-6; $RhCl(PPh_3)_3$, 14694-95-2.

Contribution from the Department of Chemistry, University of Arkansas, Fayetteville, Arkansas 72701

Iron–Oxygen Interactions in an Argon Matrix

SEIHUN CHANG, G. BLYHOLDER,*[1] and JUAN FERNANDEZ

Received July 8, 1980

The interaction of iron atoms with oxygen molecules and atoms in an argon matrix over the temperature range from 15 to 40 K has been examined. The iron atoms are produced by a hollow-cathode sputtering device. Iron–oxygen complexes are identified by oxygen-18 isotope shifts in the infrared spectra, annealing behavior, and comparison to known compounds. A band at 956 cm^{-1} is assigned to the O–O stretching frequency of a side-bonded FeO_2 structure, an assignment at variance with current literature. A band at 872 cm^{-1} is assigned to FeO while a band at 969 cm^{-1} is assigned to an Fe–O stretching mode of linear O–Fe–O. A band at 946 cm^{-1} is tentatively assigned to metastable bent O–Fe–O species which disappears upon annealing the matrix at 25 K. Oxygen atoms are formed on the surface of the matrix during its formation by the reaction of O_2 molecules with excited argon atoms from the hollow-cathode discharge. The verification of the existence of a stable FeO_2 complex which still contains an O–O bond lends credence to the proposal of a molecularly adsorbed O_2 precursor state in iron oxidation.

Introduction

The interaction of oxygen with Fe atoms is of interest because of its bearing on such diverse processes as corrosion of structural metals and oxygen transport in biological systems. There have been a number of reports on the kinetics and the surface-phase structure produced in the early stages of the interaction between a pure iron surface and oxygen.[2-10] Recent detailed examination of the kinetics of the O_2 interaction have lead to the suggestion of molecularly adsorbed O_2 as a precursor state to dissociation into immobile adsorbed oxygen atoms.[9,10] The nature of the adsorbed O_2 precursor state or the nature of the sites required to dissociate O_2, if indeed there are any requirements for O_2 dissociation, have not been discussed. In this paper the results of using matrix isolation spectroscopy to examine the initial interaction between Fe atoms and oxygen are reported and the implications with respect to oxygen adsorption on metallic iron discussed.

The interaction of oxygen with Fe atoms coordinated in biological systems has been the subject of several studies.[11-15] Infrared and Raman spectra have been interpreted[13,15] as indicating the O_2 is end bonded, as opposed to side bonded, to Fe atoms in 2+ or 3+ oxidation states. A generalized valence-bond calculation was found to favor end bonding over side bonding in an $Fe^{II}O_2$ modeling of the biological system.[16]

In contrast to these iron biological systems, a general review[17] of dioxygen in inorganic coordination complexes reveals an overwhelming preference for a side-bonded structure. For isolated iron atoms in an argon matrix one study[18] has suggested a side-bonded interaction for O_2. The reasons for Fe atoms behaving differently from Fe in iron(II) porphyrin and hemerythrin are not clear. This difference suggested to us that a more thorough study of the Fe matrix system was desirable.

The ground-state properties of molecular FeO also has been the subject of some disagreement. The Fe–O stretching frequency has been reported[18] to be at 872 ± 1 cm^{-1}. However a recent paper[19] claims it to be at 943 cm^{-1}. The value now appers to have been definitely settled[20] to be 880 cm^{-1}, and our work reported here is in agreement with this value.

Experimental Section

The cryostat used was a Cryogenic Technology Inc. Spectrim TM helium cryogenic cooler. The cold window and external windows of the vacuum system along the optical path were all potassium bromide. The temperature of the cold window was measured with use of a gold (0.07% Fe) vs. chromel thermocouple soldered on the copper window support with indium solder.

Iron atoms were produced by an electric discharge in the argon system with use of an iron foil as the cathode. The device used in

(1) To whom correspondence should be addresed.
(2) M. A. H. Lanyon and B. M. W. Trapnell, *Proc. R. Soc. London, Ser. A*, **227**, 387 (1955).
(3) M. W. Roberts, *Trans. Faraday Soc.*, **57**, 99 (1961).
(4) J. Kruger and H. T. Yolken, *Corrosion*, **20**, 296 (1964).
(5) S. Chang and W. H. Wade, *J. Phys. Chem.*, **74**, 2484 (1970).
(6) A. J. Pignocco and G. E. Pellissier, *Surf. Sci.*, **7**, 261 (1967).
(7) P. B. Sewell, D. F. Mitchell, and M. Cohen, *Surf. Sci.*, **33**, 535 (1972).
(8) C. Leygraf and S. Ekelund, *Surf. Sci.*, **40**, 609 (1973).
(9) A. M. Horgan and D. A. King, *Surf. Sci.*, **23**, 259 (1970).
(10) G. W. Simmons and D. J. Dwyer, *Surf. Sci.*, **48**, 373 (1975).
(11) J. S. Valentine, *Chem. Rev.*, **73**(3), 235 (1973).
(12) J. B. R. Dunn, D. F. Shriver, and I. M. Klotz, *Biochemistry*, **14**, 2689 (1975).
(13) J. P. Collman, R. R. Gange, C. A. Reed, T. R. Halbert, G. Lang, and W. T. Robinson, *J. Am. Chem. Soc.*, **97**, 1427 (1975).
(14) W. S. Caughey, C. H. Barlow, J. C. Maxwell, J. A. Volpe, and W. J. Wallace *Ann. N.Y. Acad. Sci.*, **244**, 1 (1975).
(15) D. M. Kurtz, Jr., D. F. Shriver, and I. M. Klotz, *J. Am. Chem. Soc.*, **98**, 5033 (1976).
(16) W. A. Goddard III and B. D. Olafson, *Proc. Natl. Acad. Sci.*, **72**, 2335 (1975).
(17) L. Vaska, *Acc. Chem. Res.*, **9**, 175 (1976).
(18) (a) S. Abramowitz, N. Acquista, and I. W. Levin, *Chem. Phys. Lett.*, **50**, 423 (1977); (b) R. F. Barrow and M. Senior, *Nature (London)*, **223**, 1359 (1969).
(19) T. C. DeVore and T. N. Gallaher, *J. Chem. Phys.*, **70**, 4429 (1979).
(20) D. W. Green, G. T. Reedy, and J. G. Kay, *J. Mol. Spectrosc.* **78**, 257 (1979).

0020-1669/81/1320-2813$01.25/0